I&EC research
Industrial & Engineering Chemistry Research

Article

Cite This: Ind. Eng. Chem. Res. 2018, 57, 5903−5913

pubs.acs.org/IECR

Dynamic Simulation Study for Boil-off Gas Minimization at Liquefied Natural Gas Exporting Terminals

Yogesh M. Kurle, Qiang Xu,* and Srinivas Palanki

Dan F. Smith Department of Chemical Engineering, Lamar University, Beaumont, Texas 77710, United States

ABSTRACT: The boil-off gas (BOG) generation at LNG (liquefied natural gas) exporting terminals is significant and should be minimized and/or recycled efficiently and effectively. In this work, the study of BOG generation, minimization, and recovery has been performed for a typical LNG plant with C3MR (propane precooled mixed refrigerant) process, storage facility, loading facility, and LNG ship with four moss-type spherical tanks. Plant-wide dynamic simulations are employed to quantify dynamic BOG generations during loading and holding mode, under various LNG temperatures at LNG exporting terminals. On the basis of multiple case studies, optimum LNG temperatures under different LNG subcooling and BOG recovery strategies have been identified for the sake of total energy consumptions. This study provides valuable information about the effect of LNG subcooling temperature on BOG generation, which would help in operating LNG plants at optimum conditions and economically minimize BOG generation and recovering BOG at LNG exporting terminals. Conceivably, the resultant benefits are not only for the environmental sustainability (reduce emissions), but also for the LNG industry sustainability (save raw materials/energy and increase productivity).

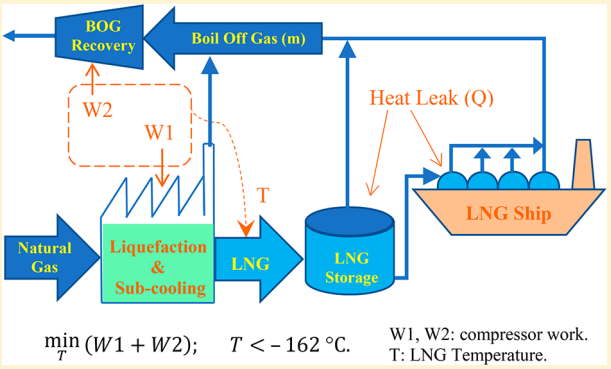

Downloaded via Qiang Xu on May 9, 2019 at 18:04:21 (UTC).
See https://pubs.acs.org/sharingguidelines for options on how to legitimately share published articles.

1. INTRODUCTION

Natural gas production and consumption are quickly growing worldwide. Comparably, natural gas is preferred over other fossil fuels due to its abandon reserves, lower prices, and cleaner burning characteristics. For the third consecutive year, the global LNG trade set a new record, reaching 258 million tonnes (MT) for 2016, which marks an increase of 13.1 MT (+5%) from 2015.[1] In 2016, the global natural gas liquefaction nameplate capacity increased by 35 MTPA (million tonnes per annum) to reach the total of 340 MTPA.[1] By January 2017, an additional 115 MTPA of liquefaction capacity was under construction worldwide, and the total proposed natural gas liquefaction capacity reached 879 MTPA.[1]

Natural gas is usually liquefied to reduce its volume and make it economical for transportation over longer distances. The LNG supply chain includes natural-gas-liquefaction plants, LNG loading/exporting terminals, LNG carriers (i.e., ships), LNG unloading/receiving terminals, and regasification facilities. The boil-off gas (BOG) is generated in all segments of the LNG supply chain—during LNG production, storage, loading, transportation, and unloading operations.[2] Among the broad scope of BOG study, this work particularly focuses on the BOG minimization at LNG exporting terminals. At an exporting terminal, three main BOG generation locations are identified: (1) BOG generated due to the flashing/depressurization of LNG from the operating pressure to storage pressure (termed as FBOG); (2) BOG generated from LNG storage tanks (termed as TBOG); and (3) BOG generated during LNG ship-loading operations (termed as Jetty BOG or JBOG).

FBOG usually exists continuously during normal operations of a natural-gas-liquefaction process. When LNG ship-loading is not in progress (called holding mode), TBOG comes out of storage tanks. When LNG ship-loading is in progress (called loading mode) and the LNG is being withdrawn from a storage tank, then the TBOG rate coming out of that storage tank would decrease and it is zero for most of the duration of the loading process. This is because the instantaneous LNG flow rate for ship-loadings is usually higher than LNG production rate (i.e., the flow rate of LNG being added to the storage tank), and thus TBOG generated is utilized to compensate the pressure drop occurred due to the net liquid outflow. Meanwhile, the makeup gas needs to be added to the storage tank during the ship-loading operation to maintain the pressure of the storage tanks at the desired value. LNG production is usually a continuous process. The ship-loading process is intermittent and may be carried out once in a few days period for each LNG train. For higher LNG production rates, multiple simultaneous ship-loading processes may occur. JBOG is not available continuously, it is available only during

Special Issue: PSE Advances in Natural Gas Value Chain

Received: August 31, 2017
Revised: November 30, 2017
Accepted: December 15, 2017
Published: December 15, 2017

© 2017 American Chemical Society

DOI: 10.1021/acs.iecr.7b03633
Ind. Eng. Chem. Res. 2018, 57, 5903−5913

LNG ship-loading process. For most of the duration of the ship-loading process, the instantaneous JBOG rate may be relatively higher than the instantaneous rate of TBOG and other BOG generation during various segments of the LNG supply chain due to the following factors: (1) ship-tanks are hotter than the LNG-being-loaded when the ship arrives at LNG loading terminals; (2) ship-tanks have a relatively higher surface area compared to LNG storage tanks with the same total volume, which causes the higher heat leak from the ambient environment; (3) heat leak into loading facilities such as pumps and pipelines during the holding mode causes additional BOG generations during the loading of LNG; and (4) LNG ship-loading rates may be higher than the rate of LNG fed to storage tanks (at exporting terminals), which result in comparatively higher rates of vapor displacement in ship tanks. Ship-loading rate is driven by keeping the ship-loading time as short as possible due to the high cost of ship demurrage.[3] Therefore, ship-loading rate is usually higher.

It should be also noted that JBOG generation is very dynamic in nature and changes with LNG loading time due to the following two factors: (1) the ship-tank temperature changes with the LNG loading time, thus heat added to LNG also changes; and (2) the LNG loading rate changes with the loading time. Initially, the LNG loading rate is kept lower to avoid thermal shocks to LNG pipelines and the ship-tanks; then the JBOG compressor capacity limits the LNG loading rate. When JBOG generation rate decreases, capacity of LNG loading lines limits the LNG loading rate. The LNG flow rate should be ramped down once ship tanks are filled up to 80% in volume.[4] Because of such dynamic operating behaviors, dynamic process simulations should be employed to help study the LNG loading process.

BOG generated during any segment of the LNG supply chain should be recovered with some recovery methods; otherwise, it must be flared, which certainly produces many green-house gases in the atmospheric environment. Note that as environmental regulations become more stringent, flaring is generally not a preferred option anymore. Meanwhile, the recovery/reuse of BOG could also help LNG industries save raw material and energy. The BOG generation in natural gas liquefaction plants and at LNG exporting/loading terminals has been discussed in many literature works. For example, Huang et al. provided methods to simulate LNG related systems and suggested use of end-flash-gas as fuel gas to run turbines in LNG plant.[5] Huang et al., in another of their publications, provided various BOG recovery strategies at LNG loading terminals, particularly for long jetties which tend to generate more JBOG due to greater heat leaks.[4] Chaker et al. stated that most publications in the past have focused on regasification terminals and have not addressed the area of liquefaction plants; thereby providing discussion on generation and management of BOG in a LNG plant, and the associated networks and machinery to manage BOG handling.[6] Wicaksono et al. studied the efficient use of recovered jetty-BOG as fuel gas using mixed-integer nonlinear programming for a fuel−gas network.[7] The effect of environmental conditions at plant locations on LNG processes has been studied in the literature. Park et al. studied the effect of ambient temperature on single-mixed refrigerant (SMR) natural gas liquefaction process and found that the specific power requirement for natural gas liquefaction decreased by 27.6% with a decrease in ambient temperature from 25 to 5 °C.[8] Jackson et al. also studied the effect of ambient temperature on LNG processes and found that LNG plants in warm locations such as North Australia and the Middle Eastern countries require 20−26% more energy than similar processes located in cold climates such as Melkoya, Norway.[9] Qyyum et al. studied effect of relative humidity of air on SMR natural-gas-liquefaction process and found that air-fin coolers are not preferred over water coolers, if relative humidity is high, due to the requirement of high compression power.[10] Several optimization studies have also been carried out on LNG processes. Ali et al. conducted an energy optimization for SMR natural gas liquefaction process using the metaheuristic vortex search algorithm.[11] Lee et al. optimized the total cost of an SMR process based on equipment cost and life expectancy.[12] Khan et al. carried out optimization of a dual mixed refrigerant (DMR) process of natural gas liquefaction.[13] Pillai et al. studied the optimum design of BOG compressor network, and stated the need for dynamic simulation of a BOG system.[14] Several BOG recovery strategies were proposed and simulated by Kurle et al. for BOG generated at an LNG plant and exporting terminals.[15] Meanwhile, overall heat transfer coefficients for LNG storage tanks and ship tanks are reported.[15] In 2016, Kurle et al. also studied the effects of ship tank temperature, tank cooling rate, and JBOG compressor capacity on JBOG generation using Aspen Dynamics simulation.[16] Namjin et al. used Aspen Dynamics to optimize operation of boil-off gas compressors, and mixed integer linear programming to decide the load distribution to different compressors.[17] Tianbiao et al. used dynamic simulation to study the stability of LNG process under disturbances of feed conditions and water-cooler temperatures.[18] Okasinski et al. used dynamic simulation to study the use of a parallel compressor string in the refrigeration cycle of C3-MR process to maintain process operation in case of failure of one of the compressors.[19,20] Okasinski et al. also used dynamic simulation to test controller strategy under conditions such as varying production rates, loss of equipment services, and loss of feed.[21] For optimization of LNG processes, Khan et al. used a sequential coordinate random search (SCRS) method to minimize compression specific power requirements.[22] Khan et al. optimized operating conditions such as mixed refrigerant (MR) composition, pressure, expansion temperature, and propane cooler temperatures for each stage.[22]

The effect of LNG temperature on BOG generation at the LNG exporting terminal has not been studied yet using dynamic simulation in order to find optimum LNG temperature for BOG minimization. In this work, the effect of LNG temperature on BOG generation is studied and the optimum temperature of LNG is identified by using dynamic process simulations. The optimum LNG temperature was found with the consideration of energy required to recover BOG and subcool LNG. Two possible locations are considered for subcooling LNG: (case 1) in the main cryogenic heat exchangers (MCHE) and (case 2) after storage tanks (at the time of ship-loading). Different values of LNG temperatures are considered for each location. The choice of each temperature is based on results of the previous temperature case. LNG temperature is decreased to observe changes in the pattern (decrease and increase) of value of total energy requirements. Energy required to subcool LNG and to recover BOG is considered for each temperature case. Two different BOG recovery methods are considered: (case A) use BOG as fuel gas, which requires BOG to be compressed to fuel gas pressure; and (case B) BOG recovered by reliquefaction,

DOI: 10.1021/acs.iecr.7b03633
Ind. Eng. Chem. Res. 2018, 57, 5903−5913

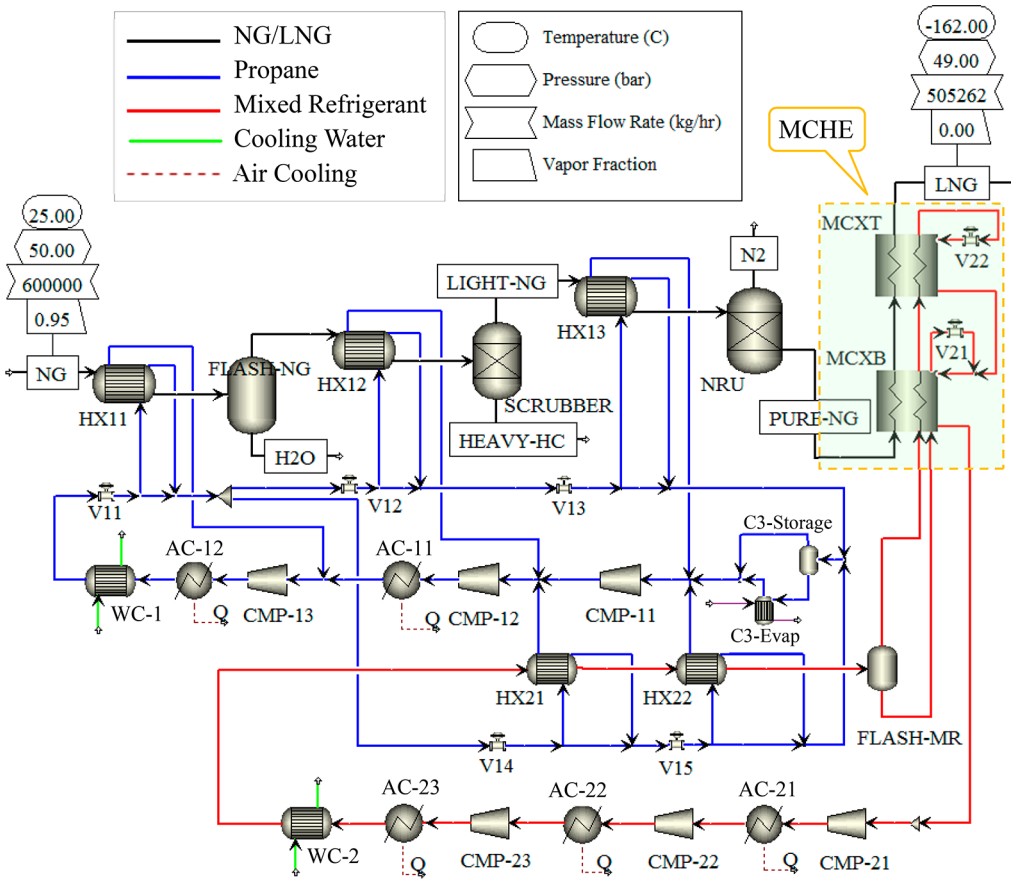

Figure 1. Steady-state simulation schematic for the LNG plant.

which requires BOG to be compressed to 50 bar and cooled to −162 °C to liquefy it. Fuel gas may be used to run gas turbines, and the fuel gas pressure requirements are specified by turbine manufacturers. Specifications for some of the gas turbines from Siemens Energy company mention fuel gas requirements from 18 to 33 bar.[23−26] The range may be wider for other gas turbines. Here, a fuel gas pressure of 30 bar is used for most of the discussions and illustrations in Figures for cases 1A and 2A. At the end, a range of optimum LNG temperature is reported for fuel gas pressure, from 10 to 50 bar. The combination of the two LNG subcooling locations (case 1 and case 2) and two BOG recovery methods (case A and case B) make a total of four cases, which can be indicated as cases 1A, 1B, 2A, and 2B. For each of four cases, an optimum LNG temperature is reported in this work. An optimum LNG temperature is defined as the LNG temperature (at particular location as considered in respective cases) at which the total energy consumption for LNG subcooling and BOG recovery is minimum.

2. PROCESS SIMULATION AND CALCULATION METHODS

A typical LNG plant, as well as LNG storage, and loading facility are simulated in Aspen Plus v10 and exported to Aspen Plus Dynamics v10.[27] On the basis of suggestions by 'Aspen Property Method Selection Assistant' in Aspen software, PR-BM (Peng−Robinson cubic equation of state with the Boston-Mathias alpha function) property method is used for the process simulation. Binary interaction parameters are called from Aspen Property Database "APV100 ASPEN-BM". The process schematic for LNG plant in steady-state simulation is shown in Figure 1. Natural gas with the flow rate of 600 000 kg/h at 25 °C and 50 bar enters the liquefaction plant. Composition (by wt %) of the feed stream is assumed to be methane 80.0, ethane 6.0, propane 2.0, *n*-butane 1.0, *i*-butane 1.0, *n*-pentane 0.5, *i*-pentane 0.5, water 5.0, and nitrogen 4.0. Propane precooled mixed-refrigerant (C3MR) liquefaction process developed by Air Products and Chemicals, Inc. is used in the study. Some of the process parameters are taken from a paper by Ravavarapu.[28] Propane is used to precool natural gas to 20, 0, and −34 °C in HX11, HX12, and HX13, respectively. Meanwhile water, heavy hydrocarbons, and excess nitrogen are removed from natural gas. Mixed refrigerant (MR) composition (by mole %) is nitrogen 10, methane 40, ethane 35, propane 15. The propane refrigeration cycle is also used to precool MR to −4 and −34 °C in HX21 and HX22, respectively. Then MR is used to liquefy natural gas in the main cryogenic heat exchanger (MCHE). The MCHE consists of bottom section (MCXB) and top section (MCXT). The LNG temperature is −115 °C in MCXB and −162 °C in MCXT. The minimum internal temperature approach (MITA) used for MCHE is 2 °C.[29] For other heat exchangers 5 °C MITA is used. Simple heat exchangers are used to represent air-coolers (denoted as AC-11, AC-21, etc. in Figure 1) after each compressor stage to cool refrigerant to 40 °C. Water-cooling (WC-1, WC-2) is used after last stage to achieve cooling to 20 °C. The LNG coming out of MCHE is at −162 °C and 49 bar with the composition (by wt %) of methane 92.8275, ethane 4.9875, propane 0.7125, *n*-butane 0.1187, *i*-butane 0.1187, *n*-pentane 0.0534, *i*-pentane 0.0534, water 0.0,

DOI: 10.1021/acs.iecr.7b03633
Ind. Eng. Chem. Res. 2018, 57, 5903−5913

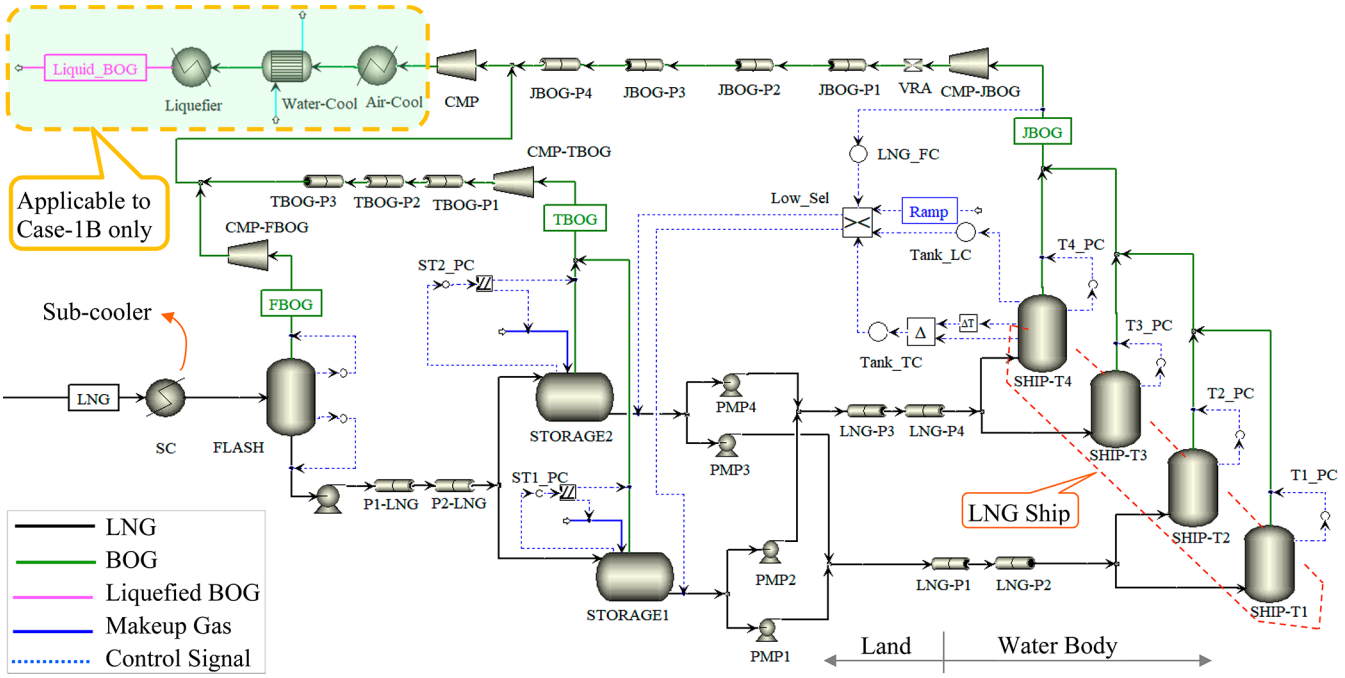

Figure 2. Dynamic simulation schematic for case 1 showing LNG subcooler, depressurization, storage facility, loading facility, ship tanks, and BOG handling facility.

and nitrogen 1.1281. This is also the composition of LNG in the subcooler for case 1, since the subcooling location for case 1 is in MCHE or immediately after MCHE. For case 2 LNG subcooling location is after the storage tanks, and the LNG is flashed in FLASH and in storage tanks before that location; therefore, the LNG composition in subcoolers in case 2 is different than that in case 1. The LNG liquefaction capacity for the studied process is 505 tonne/h, which is about 4.24 MTPA (assuming 350 operating days a year). The LNG temperature of −162 °C at the outlet of the MCHE and no further cooling duty provided at any location in the downstream is considered as the base case.

The liquefaction process is the same for both the subcooling cases discussed here. The different simulation setups regarding the LNG subcooling location for case 1 and case 2 are discussed in sections 2.1 and 2.2, respectively. The following assumptions are made:

(1) The vapor and liquid are at equilibrium in flash tanks, storage tanks and ship tanks;
(2) At any instance, the temperature of the content (LNG and BOG) of a tank is the same at each point within the tank. Heat added will be dissipated instantaneously within all content of the tank. (However, the tank wall temperature could be different from the content of the tank).

2.1. Subcooling LNG in MCHE (case 1). The process modeling schematic for the LNG subcooler, storage, loading facility, ship tanks, and BOG handling facility in dynamic simulation is shown in Figure 2. For easier calculations of energy requirements for LNG subcooling, a separate heat exchanger unit (SC) is used in the simulation. Practically, LNG can be subcooled in the MCHE itself, using the existing refrigeration cycle available for the liquefaction process. The LNG temperature can be controlled by varying mixed refrigerant composition, its amount, and pressure in the Flash-MR tank. The LNG liquefaction pressure is kept constant at a design pressure (49 bar), and only the effect of varying temperature is studied in this work. In the simulations, LNG from MCHE is cooled further in the subcooler, SC shown in Figure 2. As a parametric study, various values for the temperature of the LNG coming out of SC are considered. For the selection of the temperatures, subcooler temperature was decreased stepwise until the total energy consumption changes the pattern (for example, first decreases and then increases). LNG subcooling temperatures considered for individual case range from −162 to −169 °C. Only the energy required to cool the LNG below −162 °C is considered for the comparison, because the energy required to cool down the LNG to −162 °C is constant for all the cases. The LNG from the SC is then sent to the flash tank ("FLASH") to reduce the pressure to 1.06 bar. Then it is sent to storage tanks. The pipeline equivalent length from flash tank to storage tanks is assumed to be 1 km. Two above-ground full-containment type storage tanks with the volume capacity of 168 000 m^3 each are considered. During the LNG ship-loading process, LNG is pumped from storage tanks into ship-tanks through jetty pipelines. The pipeline equivalent length from storage tanks to LNG ship tanks is assumed to be 6 km in this study, to represent a long jetty.[4,30] There are two LNG loading lines: LNG-P1 and LNG-P2 making one loading line and LNG-P3 and LNG-P4 making another transfer line. Each loading line has an inner diameter of 24 in. and maximum loading capacity of 5000 m^3/h. The overall heat transfer coefficient of the LNG pipes is considered to be 0.26 W/(m^2·K).[31]

An LNG ship with four moss-type spherical tanks is considered in this work. Other types of LNG carriers, such as membrane type, may be studied in the future using similar methodology. Here, to represent the Moss-type ship-carrier, the ship-tanks are modeled as four flash-tanks (SHIP-T1 through SHIP-T4) with spherical geometry specification. Total capacity of the LNG ship is assumed to be about 143 000 m^3, and actual LNG loading capacity is about 140 000 m^3 (98%[32]

DOI: 10.1021/acs.iecr.7b03633
Ind. Eng. Chem. Res. 2018, 57, 5903−5913

of the total volume). For about 35 750 m^3 capacity of each ship-tank, their diameter is calculated to be about 40.4 m with additional 1 m height of the cylindrical portion at the equator. The heat leak calculations for storage tanks, pipelines, and ship-tanks are discussed in the previous work.[15] The overall heat transfer coefficient of the ship-tanks is taken as 0.11 W/(m^2·K).[15] In the simulation, environmental heat transfer and equipment heat transfer is considered for storage tanks, pipelines, and ship-tanks. In addition to the environmental heat transfer, the equipment heat transfer also causes BOG generation. The equipment heat transfer option for the ship-tanks is considered to represent the heat transfer from hotter ship-tanks into LNG. Ship-tanks are assumed to be at −125 °C at the beginning of LNG loading. The flash-tank model used to simulate the ship-tanks considers the vapor−liquid equilibrium and even-temperature-distribution throughout the contents of the the tank. A small amount of LNG is left in ship tanks (called heel) after LNG unloading at LNG receiving terminals. The heel limits rising of ship tank temperature during voyage from receiving terminal to loading terminal. 1 vol % heel is assumed in the ship-tanks at the beginning of the loading operation. For the ship tank temperature of −125 °C, the corresponding heel composition is calculated by using Aspen simulation. The heel composition (by wt %) is methane 4.76, ethane 75.88, propane 13.03, *n*-butane 2.18, *i*-butane 2.18, *n*-pentane 0.98, *i*-pentane 0.98, and nitrogen 0. The compressor (CMP-JBOG) installed on the ship sends the JBOG to the shore. An isentropic efficiency of 0.72 and mechanical efficiency of 0.9 are used for all compressors in the simulation. Vapor return arm (VRA) is assumed to have a pressure drop of 0.25 bar. JBOG-P1 and JBOG-P2 transfer JBOG from ship to storage area. JBOG-P3 and JBOG-P4 transfer JBOG from the storage area to the LNG plant/BOG recovery area. The JBOG pipe diameter is 24 in. and has overall heat transfer coefficient of 0.5 W/(m^2·K). The list of the assumed parameter values is given in Table 1. The parameter values assumed in the simulation are kept constant for all the simulation cases; therefore, the results would be reliable and comparable. Using an on-shore compressor (CMP), JBOG is compressed to fuel gas pressure (30 bar) for case 1A, and to 50 bar for case 1B. For case 1B, the compressed JBOG is cooled to 40 °C using air and then to 20 °C using water. The JBOG is liquefied to −162 °C at 49 bar in the "Liquefier".

When the radius of a pipe with insulation equals its critical radius, the heat transfer through the pipe is the maximum. The critical radius of a pipe is given by eq 1.[33] In eq 1, R_c is the critical radius of insulated pipe, k_i is the thermal conductivity of insulation, and h_a is the film heat transfer coefficient of surrounding fluid (air). The thermal conductivity of polyurethane rigid foam insulation is 0.022 W/(m·K).[34] Film heat transfer coefficient of air is 35 W/(m^2·K).[35] From eq 1, the critical radius equals 0.63 mm. In this simulation, the radius of the LNG pipes and JBOG pipes (i.e., 305 mm) is much greater than the calculated critical radius. Therefore, the issue of critical radius will not be a factor in this situation.

$$R_c = \left(\frac{k_i}{h_a}\right) \quad (1)$$

The blue dotted lines in Figure 2 show the strategy for the process control. The flash tank has a level controller and pressure controller. Split-range type controllers (ST1_PC and ST2_PC) are used for storage tanks to control pressure. The split-range controller removes vapors from the storage tank if the tank pressure is greater than the set point (1.06 bar), and it adds makeup gas if the tank pressure is lower than the set point. It is assumed that the makeup gas is available in the plant and it has a temperature of −162 °C and composition (by wt %) of methane 86 and nitrogen 14. This composition is approximately the same as the TBOG composition (for the base case). Four ship-tanks have pressure controllers to maintain pressure of 1.06 bar. The remaining process control schematic is for the LNG ship-loading process. LNG loading rate is constrained by LNG loading line capacity, JBOG compressor capacity, ship-tank level, and maximum allowed cooling-rate for the wall of the ship tanks. The LNG loading rate is the only manipulated variable for the constraints mentioned here. The LNG flow rate is adjusted by LNG_FC in order to maintain JBOG flow rate within compressor capacity limit. The compressor capacity is assumed to be 80 000 kg/h. Tank_TC reads the cooling rate of the tanks by comparing current tank temperature with the temperature 20 min in the past. Maximum cooling rate is set to 3 degrees per 20 min (based on reference of 10 °C per hour).[36] The tank-cooling-rate is maintained within the limits by Tank_TC by adjusting LNG flow rate. When the LNG level reaches 80 vol % of the ship tanks, The LNG loading rate is ramped down by using a program script "Ramp". The Low_Sel chooses the lowest value out of all the controllers' outputs. The lowest LNG flow rate at any instance would satisfy all the constraints specified above. The output signal of Low_Sel is connected to liquid outlet of two storage tanks to control the LNG loading rate.

Table 1. List of Assumed Constant Parameters

process unit/ description	parameter	assumed value	units
LNG loading lines (2 numbers)	pipeline length	6000	m (each)
LNG loading lines (2 numbers)	maximum loading capacity	5000	m^3 (each)
ship-tanks	initial temperature	−125	°C
LNG pipeline (P1-LNG and P2-LNG)	length from plant to storage area	1000	m (total)
storage tanks	number of above ground full containment type cylindrical storage tanks	2	number
storage tanks (2 numbers)	volume	168 000	m^3 (each)
ship tanks	number of moss type spherical tanks	4	number
ship tanks (4 numbers)	volume	143 000	m^3 (total)
MCHE (LNG liquefaction)	outlet pressure	49	bar
makeup gas	temperature (@ 1.06 bar)	−162	°C
makeup gas	composition	86% methane, 14% nitrogen	wt %
vapor return arm	pressure drop	0.25	bar
JBOG Pipeline	overall heat transfer coefficient	0.5	W/(m^2·K)
JBOG compressor on ship	flow capacity	80,000	kg/h
JBOG compressor on ship	outlet pressure	2.5	bar
all compressors	mechanical efficiency	0.9	
all compressors	isentropic efficiency	0.72	

DOI: 10.1021/acs.iecr.7b03633
Ind. Eng. Chem. Res. 2018, 57, 5903−5913

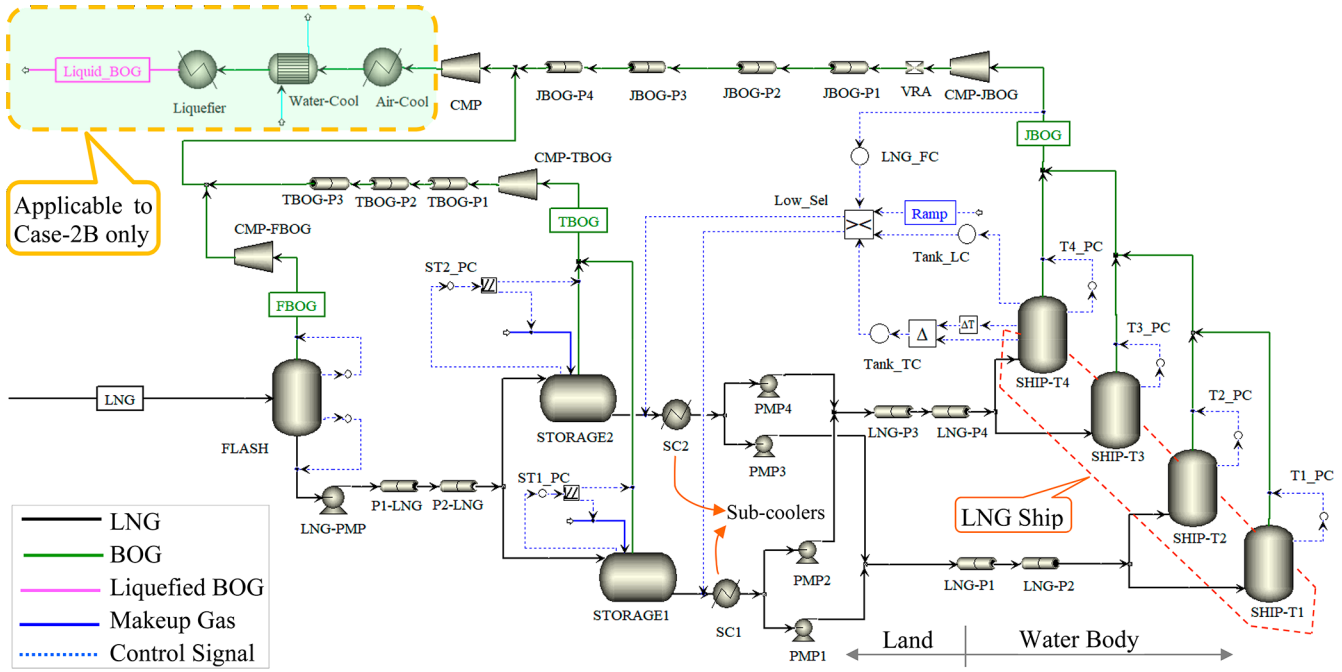

Figure 3. Dynamics simulation schematic for case 2 showing LNG depressurization, storage, LNG subcooler, loading facility, ship tanks, and BOG handling facility.

As shown in Figure 2, a simple heat exchanger model from the Aspen simulation tool is used, instead of a completed refrigeration loop, to calculate cooling duty to subcool LNG (in SC) and to liquefy JBOG (in the Liquefier unit). The actual energy required by refrigerant compressors to achieve this cooling duty can be calculated using typical values of coefficient of performance (COP) of the refrigeration cycle. Therefore, the simulation results can be applied to different refrigeration cycles by using the following equation:

$$\text{compressor work} = \left(\frac{\text{cooling duty}}{\text{COP}}\right) \tag{2}$$

The COP of the C3MR refrigeration cycle is reported as 2.13 and that for the Cascade refrigeration cycle as 1.26.[37] Another value of 1.795 for the COP of typical C3MR process is reported.[38] A COP value of 2 is used for the calculations of energy requirements and illustrations in the plots. However, a range of optimum LNG temperatures is also given for the COP range of 1 to 5. Since a simple heat exchanger and various COP values are considered, the COP of the current refrigeration loop (C3MR) in this simulation would have no effect on obtained results. Isolating the used refrigeration loop in this way makes the results valid for a wide range of refrigeration cycles. Dynamic simulations of the LNG loading process were run with different LNG temperatures for each of case 1 and case 2. During calculations, two strategies for BOG recovery are considered: (A) use of BOG as fuel gas, and (B) liquefaction of BOG. Figure 2 shows BOG compression as well as liquefaction units, which represent case 1B. For case 1A, the liquefaction unit is ignored. For case 1A, the total energy required would be energy required to subcool LNG and energy required to compress BOG to fuel gas pressure (30 bar). The total energy required for case 1B would be the addition of energy required for LNG subcooling, BOG compression to 50 bar, and BOG liquefaction.

2.2. Subcooling LNG after Storage Tanks, At the Time of Ship-Loading (Case 2). The process modeling schematic for LNG flash-tank, storage tanks, LNG subcooler, loading facility, ship tanks, and BOG handling facility in a dynamic simulation is shown in Figure 3. In case 2, the subcooling location is different than that in case 1. In case 2, LNG is subcooled at the time of LNG ship-loading, that is, after storage tanks. The liquid outlet (LNG) from two storage tanks is at 1.06 bar and −161.66 °C temperature (saturated liquid). The corresponding LNG composition (by wt %) is methane 93.01, ethane 5.10, propane 0.73, *n*-butane 0.12, *i*-butane 0.12, *n*-pentane 0.06, *i*-pentane 0.06, and nitrogen 0.8. This composition is the same as in the base case simulation at this location. LNG subcooling temperatures considered for individual cases range from −162 to −167 °C. In case 2, only the energy required to cool LNG below −161.66 °C is considered for the calculations. The LNG temperature of −161.66 °C in storage tanks is in the base case where LNG temperature at the outlet of MCHE is −162 °C and no further cooling duty provided. In Figure 3, SC1 and SC2 are the two subcoolers used to subcool LNG at the time of ship-loading. The subcooled LNG is loaded into ship-tanks. The other process units, their specifications, and procedures followed are the same as in case 1 explained in section 2.1.

3. RESULTS AND DISCUSSIONS

Saturated liquid boils upon the addition of a small amount of heat and vapors are generated. Conversely, subcooled liquid has the ability to absorb some heat before it starts boiling. BOG generation is mainly due to heat leak into LNG from the environment, hotter tanks, and hotter pipelines. BOG generation due to heat leak should decrease when LNG is subcooled. The decrease in the amount of BOG results in a decrease in energy required to recover BOG. However, the energy required to subcool LNG increases with a decrease in LNG temperature. Because of the opposite effect of the two

DOI: 10.1021/acs.iecr.7b03633
Ind. Eng. Chem. Res. 2018, 57, 5903−5913

quantities on energy consumption, there is a trade-off/optimum-value for LNG temperature at which the total energy requirement would be minimum.

For all cases, the BOG quantities shown in the plots are for one cycle of holding and loading mode (unless specified otherwise). One cycle is defined as the duration of one loading mode plus duration of one consecutive holding mode. Please note that, in case 1, the pressure of LNG in subcooler (SC) is 49 bar; and in case 2, the pressure of LNG in subcoolers (SC1 and SC2) is 1.06 bar. The difference in pressure is due to the different location of subcooling. The results for case 1 and case 2 are discussed in section 3.1 and 3.2, respectively.

3.1. Subcooling LNG in MCHE (Case 1). Figure 4 shows FBOG and TBOG quantities with respect to LNG temperature. Because of the subcooling effect, the FBOG and TBOG decrease. At about −164 °C, FBOG is negligible; and at −166.5 °C, TBOG is also suppressed. Because of suppressing FBOG and TBOG, relatively higher amounts of lighter components (mainly nitrogen) are retained in LNG. Consequently, LNG composition in storage tanks changes for each temperature case. For lower temperature, more lighter components are present in stored LNG. This results in relatively higher amount of JBOG during LNG ship-loading, even though the LNG temperature is decreasing as shown in Table 2. However, the increase in JBOG is observed to be less than 1% when subcooled from −162 °C to −169 °C. Figure 5 shows JBOG quantity in tonnes/loading for each LNG temperature case. Table 2 shows the composition of liquid in storage tank for each temperature case. Makeup gas temperature and composition chosen is approximately the same as base case TBOG temperature and composition. It contains 14% nitrogen and 86% methane by weight. Therefore, the addition of makeup gas also affects LNG in storage tanks, since vapor−liquid equilibrium is considered in this simulation. In Table 2, it shows that the subcooling LNG before FLASH affects slightly the LNG in the storage tank. The cold energy is utilized to suppress FBOG and TBOG. For some temperature cases, LNG in the storage tanks is colder than the makeup gas temperature. The quantity of makeup gas required to maintain 1.06 bar pressure in storage tank increases with decrease in the LNG temperature, as shown in Figure 6. Portion of makeup gas gets absorbed into the liquid phase due to equilibrium. This adds more nitrogen to LNG. Thus, the JBOG is not actually decreasing with LNG temperature. Instead, the JBOG is slightly increasing with decrease in the LNG temperature. This is mainly due to suppressing FBOG and TBOG, and also due to makeup gas composition. If the makeup gas with pure methane or very high content of methane and very low nitrogen is chosen, then more makeup gas is needed, since more of it will get condensed at relatively lower temperatures inside the tank. If LNG is subcooled below −166.5 °C, there is need of makeup gas even in holding mode to maintain storage tank pressure.

Figure 7 shows the energy requirement in case 1A, for subcooling LNG, BOG compression to 30 bar, and total (addition of the first two) energy requirement. Energy consumption to subcool LNG increases with a decrease in LNG temperature. Corresponding total BOG quantity decreases up to about −166.5 °C temperature, thus the energy required to recover BOG also decreases from 1882 to 1071

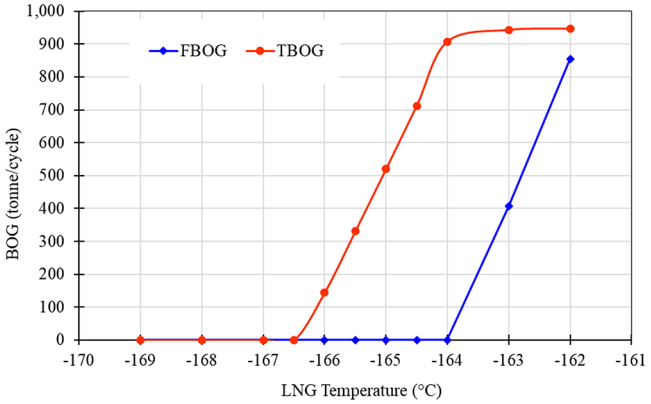

Figure 4. FBOG and TBOG for different LNG temperatures (case 1).

Table 2. Properties of LNG in Storage Tanks for Case 1

LNG temp after subcooler (°C)	temp (°C)	methane (wt %)	ethane (wt %)	nitrogen (wt %)
−162	−161.65	93.01	5.11	0.8
−163	−161.75	92.98	5.07	0.87
−164	−161.86	92.93	5.04	0.96
−165	−161.97	92.88	5.01	1.05
−166	−162.09	92.82	4.98	1.14
−167	−162.21	92.77	4.95	1.23
−168	−162.31	92.73	4.92	1.31
−169	−162.41	92.69	4.89	1.39

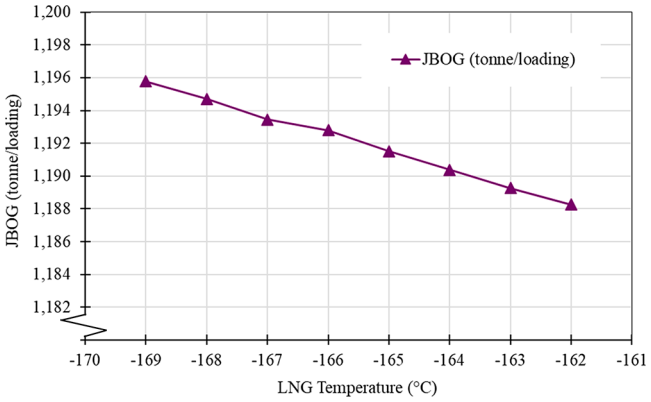

Figure 5. Amount of JBOG per LNG ship-loading for different LNG temperatures (case 1).

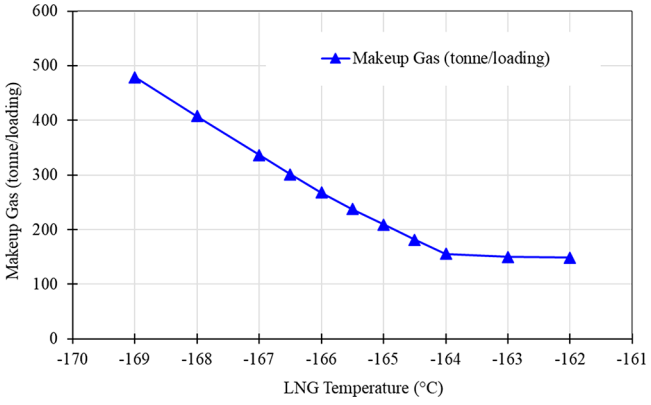

Figure 6. Makeup gas requirement for two storage tanks during LNG ship-loading (case 1).

DOI: 10.1021/acs.iecr.7b03633
Ind. Eng. Chem. Res. 2018, 57, 5903−5913

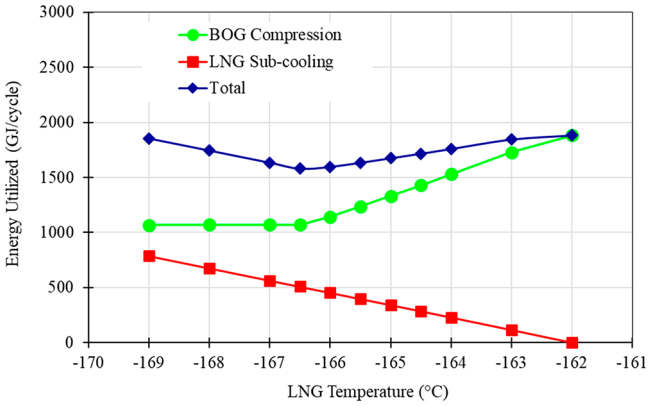

Figure 7. Energy consumption for case 1A with respect to LNG temeprature.

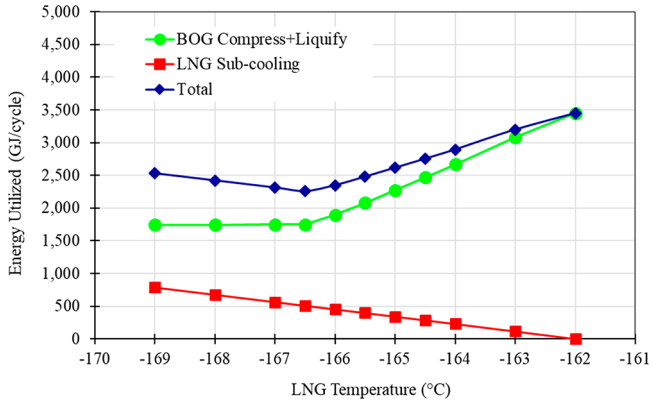

Figure 8. Energy consumption for case 1B with respect to LNG temperature.

GJ/cycle. When FBOG and TBOG are suppressed completely, there is no significant change in the total BOG quantity. Below −166.5 °C, total BOG quantity stays practically the same. Therefore, the energy required for LNG subcooling is increasing but the energy required to recover the BOG is constant. This results in an increase in total energy consumption below −166.5 °C. The values for energy consumption at optimum points are summarized in Table 3 for all cases and compared to the base case. Figure 8 shows the energy requirements in case 1B, that is, for subcooling LNG, BOG recovery by liquefaction (i.e., BOG compression to 50 bar and BOG liquefaction), and total energy requirement. For this case also, the total energy requirement decreases with a decrease in LNG temperature up to −166.5 °C. The BOG recovery energy decreases from 3449 to 1750 GJ/cycle, which is 1699 GJ/cycle energy savings in BOG recovery. Out of this, 508 GJ/cycle is required for LNG subcooling; thus, the net energy saving is 1191 GJ/cycle. This is about 35% of base case energy consumption. A COP of 2 is used for the values in the plots. The optimum point of −166.5 is the same for any COP from 1 to 5. If the amount of FBOG and TBOG available is more than needed (as fuel gas), then LNG may be subcooled in MCHE to reduce BOG recovery cost.

3.2. Subcooling LNG at the Time of Ship Loading (Case 2). The difference between case 1 and case 2 should be noted. In case 1, the composition of LNG being loaded changes with each temperature case. This change is due to suppression of FBOG and TBOG by subcooling LNG, and mixing of the makeup gas with LNG in storage tanks. However, in case 2, LNG is subcooled after storage tanks, and FBOG and TBOG are not changing, thus the composition of LNG being loaded stays constant. Since only one parameter is changing in case 2, which is the temperature of LNG being loaded, the effects of LNG subcooling on JBOG generation can be compared easily. Figure 9 shows the amount of JBOG per ship loading for each temperature case in case 2. JBOG generation decreases from an LNG temperature of −161.66 to −165 °C. JBOG generation for LNG subcooled below −165 °C remains practically the same. Mainly, the vapor displacement in ship tanks contributes toward the JBOG generation at lower LNG temperatures. The total JBOG generation (due to all factors) decreases from 1190 tonnes to 244 tonnes per loading until the LNG temperature is about −165 °C, after which it roughly remains the same.

Figure 10 shows energy consumption for case 2A, where total BOG is compressed to 30 bar to use as fuel gas. Even though JBOG is not available during holding mode, the energy required to compress FBOG and TBOG to 30 bar during holding mode is added to calculate the total energy required. The amount of energy required to subcool LNG increases with

Table 3. BOG Quantities and Energy Consumption for Each Case at Optimum Temperature, and Comparison with Base Case

		corresponding BOG (tonnes/cycle)			energy requirement[b] (GJ/cycle)				energy savings[b] (GJ/cycle)	net energy savings[b] (GJ/cycle)	
	optimum LNG temp[a] (°C)	FBOG	TBOG	JBOG	*a*	*b*	*c*	*d*	*e*	*f*	net energy savings (%)
base case (A)		855	947	1188	0	851	1031	1882			
case 1A	−166.5	≈0	≈0	1193	508	≈0	1071	1579	811	303	16
case 2A	−164.0	855	947	327	269	851	358	1478	673	404	21
base case (B)		855	947	1188	0	1741	1708	3449			
case 1B	−166.5	≈0	≈0	1193	508	≈0	1750	2258	1699	1191	35
case 2B	−164.75	855	947	253	355	1741	441	2537	1267	912	26

[a]At the location where LNG is being subcooled. Corresponding LNG pressure for case 1 is 49 bar and that for case 2 is 1.06 bar. [b]Notation: *a* = energy required to subcool LNG below −162 °C for case 1, or below −161.66 for case 2; *b* = energy required to recover FBOG and TBOG during loading as well as holding mode; *c* = energy required to recover JBOG; *d* = total energy requirement = *a* + *b* + *c*; *e* = savings in the energy required for BOG recovery = [(*b* + *c*) for respective base case] − [(*b* + *c*) for optimized case]; *f* = net energy savings = *e* − *a*. Note: Results in this table are for the following conditions only: For case 1A and case 2A, fuel gas pressure is 30 bar and COP of LNG subcooler is 2. For case 1B and case 2B, compression pressure is 50 bar, and COP of LNG subcooler as well as BOG liquefier is 2.

DOI: 10.1021/acs.iecr.7b03633
Ind. Eng. Chem. Res. 2018, 57, 5903−5913

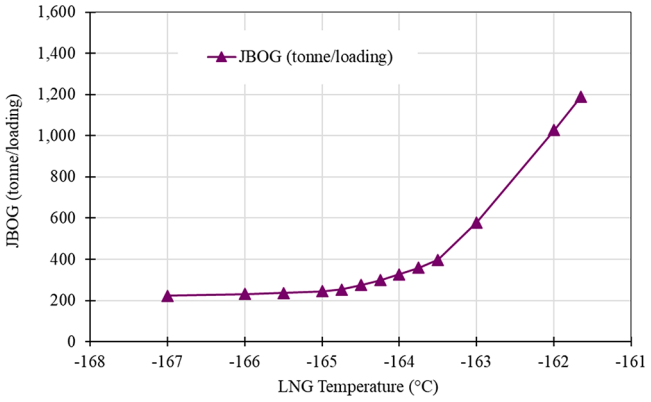

Figure 9. Amount of JBOG per LNG ship loading for different LNG temperatures (case 2).

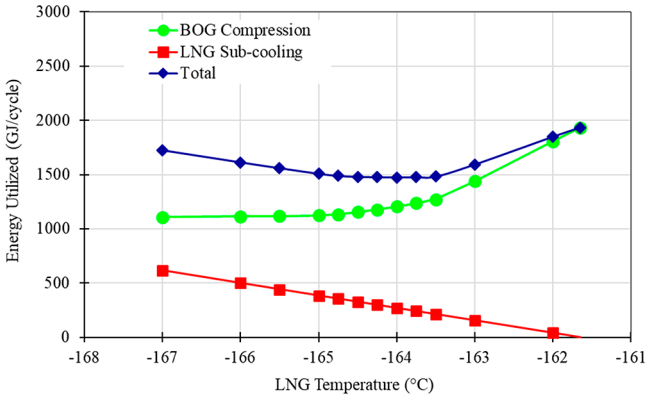

Figure 10. Energy consumption for case 2A with respect to LNG temperature.

degree of subcool. As the effect of LNG subcooling, the amount of JBOG decreases; thus, energy required to compress JBOG also decreases. The total energy consumption for this case decreases to 1478 GJ when the LNG temperature is about −164 °C. Below this temperature, the decrease in energy required for JBOG recovery is smaller than the increase in energy required for the LNG subcooling. Therefore, the total energy consumption starts increasing as the LNG is subcooled below −164 °C.

Figure 11 illustrates energy requirements for case 2B. In this case, JBOG and also FBOG and TBOG are recovered by

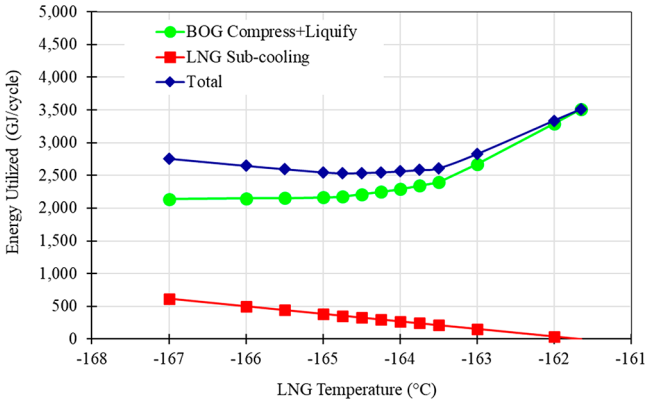

Figure 11. Energy consumption for case 2B with respect to LNG temperature.

reliquefaction, which requires compression to 50 bar as well as cooling to −162 °C. This results in more energy consumption per unit total BOG quantity for its recovery as compared to case 2A. Thus, the decrease in JBOG compensates the energy required for LNG subcooling at temperatures lower than that in case 2A (−164 °C). The energy required for total BOG liquefaction for a complete cycle decreases from 3449 to 2537 GJ due to a decrease in the amount of JBOG as the LNG temperature decreases from −161.66 °C to −164.75 °C. For a COP of 2, the lowest total energy requirement is observed for the LNG temperature of about −164.75 °C.

Lastly, range of optimum LNG temperature is given in Table 4 for the range of fuel gas pressure from 10 to 50 bar and the range of COP value from 1 to 5. For case 1A and case 1B the optimum temperature is the same −166.5 °C. This is because FBOG and TBOG become nearly zero at −166.5 °C, and below this temperature the total BOG starts increasing due to an increase in JBOG. For higher fuel gas pressure requirements and higher COP values, it is relatively more economic to subcool LNG and suppress BOG to save BOG recovery costs. The same value of COP is considered for refrigeration used for subcooling LNG and that for liquefying BOG. For very low values of fuel gas pressure (for example, 10 bar) it is not economic to subcool LNG. The same is true for a COP below 1.25. This is with the assumption that BOG is generating extra utility and there is some other fuel gas supply available to meet fuel gas demands of the plant (for example, to run gas turbines).

For case 2A, the optimum LNG temperature ranges from −163.5 to −164.5 for fuel gas pressure between 10 to 50 bar, with consideration of COP value of 2. For COP ranging from 1 to 5, the optimum LNG temperature for case 2A and 30 bar fuel gas pressure is between −163.5 and −164.75 °C. For COP ranging from 1 to 5, the optimum LNG temperature for case 2B is between −164 and −165 °C. The range of corresponding total energy requirements are also listed in Table 4. JBOG is available intermittently (only during LNG ship-loading) and results in disturbances in the BOG recovery system. If BOG is being utilized as fuel gas, it is usually desired to have the BOG available continuously and with minimum fluctuations. In this case, LNG shall be subcooled after storage tanks (during ship loading) to minimize JBOG; whereas FBOG and TBOG shall be maintained for supply of fuel gas.

The mixed refrigerant composition may be adjusted to get the amount of subcooling required to achieve LNG optimum temperature. BOG recovery avoids waste of material and energy, and flaring. Efficient recovery of BOG minimizes recovery cost and avoids energy waste. Subcooling LNG reduces BOG at the exporting terminal as well as BOG generated during transportation.

4. CONCLUSIONS

On the basis of this study, the optimum LNG temperature for case 1 (subcooling LNG in MCHE) is −166.5 °C for both BOG recovery cases considered. The values may be affected by composition and temperature of the makeup gas being used to maintain storage tank pressure, and it may also vary with LNG composition. Subcooling LNG in MCHE suppresses FBOG and TBOG predominantly; whereas subcooling it after storage tank (at the time of LNG ship-loading) suppresses JBOG. The optimum temperature for case 2A is −164 and that for case 2B is −164.75 °C. The energy savings are between 16 to 35% of BOG recovery energy, for different cases, with fuel gas pressure

DOI: 10.1021/acs.iecr.7b03633
Ind. Eng. Chem. Res. 2018, 57, 5903−5913

Table 4. Range of Optimum LNG Temperature (°C) and Corresponding Total Energy Consumption (GJ/cycle) for Range of Parameter Values

BOG compression pressure (bar)	COP	case 1A	case 1B	case 2A	case 2B
10 to 50	2	−166.5[a] [1144 to 1795]		−163.5 to −164.5 [969 to 1746]	
30	1 to 5	−166.5[b] [1882 to 1275]		−163.5 to −164.75 [1695 to 1275]	
50	1 to 5		−166.5 [3231 to 1675]		−164.0 to −165.0 [3642 to 1850]

[a](Exception) It is not economic to subcool LNG if fuel gas pressure requirement is below ∼15 bar. [b](Exception) It is not economic to subcool LNG if COP for refrigerant cycle used in subcoolers is below ∼1.25. Note: The range of total energy consumption (GJ/cycle) is given in brackets. In case 1B and case 2B, the same COP value is considered at a time for both LNG subcooler(s) and BOG-liquefier. In case 1B and case 2B BOG compression pressure is fixed to 50 bar. The variation in pressure applies only to case 1A and case 2A. For case 1A and case 2A, COP applies to only LNG subcooler(s).

of 30 bar and COP of 2. Even though every LNG plant is not the same, the methodology from this work can be applied to calculate the optimum LNG temperature to minimize energy consumption for the BOG recovery at LNG exporting terminals. Conceivably, the resultant benefits are not only for environmental sustainability (reduce emissions), but also for LNG industry sustainability (save raw materials/energy and increase productivity).

It should be highlighted that the objective of this work was to study the effect of LNG temperature on BOG generation and recovery at LNG exporting terminals. Practical application of the work must be assessed based on safety, regulation policies, and other such critical factors. The storage and transportation of subcooled liquid must be very carefully monitored and controlled, because it is very important to maintain the pressure of the containers within limits of design-pressure. For storage and transportation of subcooled LNG, there is the possibility of developing negative pressure in the storage tanks and ship tanks,[39] and it is necessary to consider innovative solutions to store and transport subcooled liquids.[40,41] If regulations permit, and adequate safety can be practiced, storage and transport of subcooled LNG should be economically beneficial to reduce BOG generation.

AUTHOR INFORMATION

Corresponding Author

*Tel.: 409-880-7818. Fax: 409-880-2197. E-mail: Qiang.xu@lamar.edu.

ORCID

Yogesh M. Kurle: 0000-0001-7345-6074

Qiang Xu: 0000-0002-2252-0838

Notes

The authors declare no competing financial interest.

ACKNOWLEDGMENTS

This work was supported in part by Center for Advances in Port Management, Lamar University Visionary Initiative Project, and Anita Riddle Faculty Fellowship.

ABBREVIATIONS

BOG	boil-off gas
C3	propane
C3MR	propane precooled mixed refrigerant process (natural gas liquefaction process)
COP	coefficient of performance (for refrigeration cycle)
FBOG	boil-off gas from depressurization of LNG after MCHE
JBOG	boil-off gas from jetty (while loading LNG into ship-tanks)
LNG	liquefied natural gas
MCXB	main cryogenic heat exchanger bottom section
MCHE	main cryogenic heat exchanger (MCXB and MCXT)
MCXT	main cryogenic heat exchanger top section
MR	mixed refrigerant
MTPA	million tonnes per annum
N_2	nitrogen
NG	natural gas
NRU	nitrogen removal unit
TBOG	boil-off gas from LNG storage tanks
VRA	vapor return arm

REFERENCES

(1) Carroll, D. *IGU World LNG Report−2017 Edition*; International Gas Union, 2017; pp 4−5.

(2) Dobrota, Đ; Lalić, B.; Komar, I. Problem of Boil - off in LNG Supply Chain. *Trans. Marit. Sci.* **2013**, *2*, 91−100.

(3) Coyle, D.; Durr, C.; Shah, P. *LNG: A Proven Stranded Gas Monetization Option* **2003**, No. SPE-84251-MS, DOI: 10.2118/84251-MS.

(4) Huang, S.; Hartono, J.; Shah, P. BOG Recovery from Long Jetties During LNG Ship-Loading. 15th, International Conference and Exhibition on Liquefied Natural Gas (LNG15); Gas Technology Institute, Barcelona, Spain, 2007; Vol. 2, pp PO−34.1.

(5) Huang, S.; Tsai, N.; Oliver, S. Simple and Versatile Methods for Modeling LNG-related systems. 88th Annual Convention of the Gas Processors Association 2009:2009 GPA Convention: Enhancing Midstream's Voice; Gas Processors Association (GPA), 2009; Vol. *1*.

(6) Chaker, M.; Meher-Homji, C. B.; Pillai, P.; Bhattacharya, D.; Messersmith, D. Application of Boil Off Gas Compressors in LNG Plants; Oil and Gas Applications; ASME Turbo Expo 2014: Turbine Technical Conference and Exposition: Dusseldorf Germany, 2014; Vol. *3B*, pp V03BT25A021.10.1115/GT2014-27076

(7) Wicaksono, D. S.; Karimi, I. A.; Alfadala, H.; Al-Hatou, O. I. Integrating Recovered Jetty Boil-off Gas as a Fuel in an LNG Plant. *17th European Symposium on Computer Aided Process Engineering−ESCAPE17*; Plesu, V., Agachi, P. S., Eds.; Elsevier, 2007.

(8) Park, K.; Won, W.; Shin, D. Effects of varying the ambient temperature on the performance of a single mixed refrigerant liquefaction process. *J. Nat. Gas Sci. Eng.* **2016**, *34*, 958−968.

(9) Jackson, S.; Eiksund, O.; Brodal, E. Impact of Ambient Temperature on LNG Liquefaction Process Performance: Energy Efficiency and CO2 Emissions in Cold Climates. *Ind. Eng. Chem. Res.* **2017**, *56*, 3388−3398.

(10) Qyyum, M. A.; Minh, L. Q.; Ali, W.; Hussain, A.; Bahadori, A.; Lee, M. Feasibility study of environmental relative humidity through

DOI: 10.1021/acs.iecr.7b03633
Ind. Eng. Chem. Res. 2018, 57, 5903−5913

the thermodynamic effects on the performance of natural gas liquefaction process. *Appl. Therm. Eng.* **2018**, *128*, 51−63.
(11) Ali, W.; Qyyum, M. A.; Qadeer, K.; Lee, M. Energy optimization for single mixed refrigerant natural gas liquefaction process using the metaheuristic vortex search algorithm. *Appl. Therm. Eng.* **2018**, *129*, 782−791.
(12) Lee, I.; Moon, I. Total Cost Optimization of a Single Mixed Refrigerant Process Based on Equipment Cost and Life Expectancy. *Ind. Eng. Chem. Res.* **2016**, 55, 10336−10343.
(13) Khan, M. S.; Karimi, I. A.; Lee, M. Evolution and optimization of the dual mixed refrigerant process of natural gas liquefaction. *Appl. Therm. Eng.* **2016**, *96*, 320−329.
(14) Pillai, P.; Messersmith, D.; Yao, J.; Chaker, M.; Meher-Homji, C. Boil Off Gas Optimization in LNG Liquefaction Plants. 92nd Annual GPA (Gas Processors Association) Convention; San Antonio, TX, USA, 2013.
(15) Kurle, Y. M.; Wang, S.; Xu, Q. Simulation study on boil-off gas minimization and recovery strategies at LNG exporting terminals. *Appl. Energy* **2015**, *156*, 628−641.
(16) Kurle, Y. M.; Wang, S.; Xu, Q. Dynamic simulation of LNG loading, BOG generation, and BOG recovery at LNG exporting terminals. *Comput. Chem. Eng.* **2017**, *97*, 47−58.
(17) Jang, N.; Shin, M. W.; Choi, S. H.; Yoon, E. S. Dynamic Simulation and Optimization of the Operation of Boil-Off Gas Compressors in a Liquefied Natural Gas Gasification Plant. *Korean J. Chem. Eng.* **2011**, *28* (5), 1166−1171.
(18) He, T.; Ju, Y. Dynamic simulation of mixed refrigerant process for small-scale LNG plant in skid mount packages. *Energy* **2016**, *97*, 350−358.
(19) Okasinski, M. J.; Liu, Y. N. Dynamic Simulation of C3-MR LNG Plants with Parallel Compression Strings. http://www.airproducts.com/~/media/Files/PDF/industries/lng/lng-dynamic-simulation-c3-mr-lng-plants.pdf (accessed November, 2017).
(20) Okasinski, M. J.; Bhadra, S.; Johnston, B. Recommendations for Restarting a Parallel Compressor String Based on Dynamic Simulation. http://www.airproducts.com/~/media/Files/PDF/company/company-overview/news-center/LNG18-restart-methods.pdf (accessed November, 2017).
(21) Okasinski, M. J.; Schenk, M. A. Dynamics of Baseload Liquefied Natural Gas Plants—Advanced Modelling And Control Strategies. http://www.ivt.ntnu.no/ept/fag/tep4215/innhold/LNG%20Conferences/2007/fscommand/PO_31_Okasinski_s.pdf (accessed November, 2017).
(22) Khan, M. S.; Karimi, I. A.; Bahadori, A.; Lee, M. Sequential coordinate random search for optimal operation of LNG (liquefied natural gas) plant. *Energy* **2015**, *89*, 757−767.
(23) Siemens Energy SGT-500 Industrial Gas Turbine https://www.energy.siemens.com/us/pool/hq/power-generation/gas-turbines/SGT-500/downloads/SGT-500_for_PG_EN.pdf (accessed November, 2017).
(24) Siemens Energy SGT-600 Industrial Gas Turbine. https://www.energy.siemens.com/co/pool/hq/power-generation/gas-turbines/SGT-600/downloads/SGT-600_GT_PowerGen_EN.pdf (accessed November, 2017).
(25) Siemens Energy SGT-700 Industrial Gas Turbine. https://www.energy.siemens.com/nl/pool/hq/power-generation/gas-turbines/SGT-700/Brochure_Siemens_Gas-Turbine_SGT-700_PG.pdf (accessed November, 2017).
(26) Siemens Energy Siemens Gas Turbine Package SGT5-PAC 4000F. https://www.energy.siemens.com/co/pool/hq/power-generation/gas-turbines/SGT5-4000F/sgt5-4000f-application-overview.pdf (accessed November, 2017).
(27) *Aspen Plus Dynamics*; Aspen Technology Inc., 2015; Vol. *8.8*.
(28) Ravavarapu, V. N.; Oakley, J. H.; White, C. C. Thermodynamic Analysis of a Baseload LNG Plant. *Chemeca 96: Excellence in Chemical Engineering; 24th Australian and New Zealand Chemical Engineering Conference and Exhibition; Proceedings*; Weiss, G., Ed.; Institution of Engineers: Australia, 1996: Vol. *1*, pp 143−148, no. 96/13.
(29) Aspelund, A.; Gundersen, T.; Myklebust, J.; Nowak, M. P.; Tomasgard, A. An Optimization-Simulation Model for a Simple LNG Process. *Comput. Chem. Eng.* **2010**, *34*, 1606−1617.
(30) Huang, S.; Kotzot, H.; Vega, F.; Durr, C. Selecting the Optimal Scheme for N2 Injection in an LNG Terminal. Gas Processors Association, 84th Annual Convention; San Antonio, Texas, March 13−16, 2005.
(31) Kitzel, B. *Choosing the right insulation*. www.phpk.com/pdf/LNGIndustry2008.pdf (accessed February 15, 2015).
(32) International Maritime Organization. *International Code for the Construction and Equipment of Ships Carrying Liquefied Gases in Bulk (IGC Code)*; Witherby Seamanship International, 1994; MSC.32(63), Amendments: Chapter 15−Filling limits for cargo tanks.
(33) Kern, D. Q. *Process Heat Transfer*; McGraw-Hill Book Company, 1950; pp 871.
(34) Jarfelt, U.; Ramnas, O. Thermal conductivity of polyurathane foam−best performance. 10th International Symposium on District Heating and Cooling, Hanover, Germany, 2006, section *6a*.
(35) EngineeringToolbox.com Convective Heat Transfer Coefficient of Air. https://www.engineeringtoolbox.com/convective-heat-transfer-d_430.html (accessed November, 2017).
(36) McGuire, G.; White, B. *Liquefied Gas Handling Principles On Ships and in Terminals*; Witherby & Co Ltd: London EC1R 0ET, England, 2000; pp 308−163.
(37) Yoon, J.; Lee, H.; Oh, S.; Lee, S.; Choi, K. Characteristics of Cascade and C3MR Cycle on Natural Gas Liquefaction Process. *Int. J. Chem. Mol. Eng.* **2009**, *3*, 620.
(38) Nezhad, S. A.; Shabani, B.; Soleimani, M. Thermodynamic Analysis of Liquefied Natural Gas (LNG) Production Cycle in APCI Process. *J. Therm. Sci.* **2012**, *21*, 564.
(39) Scurlock, R. LNG/LPG and cryogenics. https://www.gasworld.com/lng/lpg-and-cryogenics/2971.article (accessed August, 20, 2017).
(40) Aronson, D. Vessel for subcooled liquid. U.S. Patent US3045437 A, 1962.
(41) James, M.; Maher, J. B. Apparatus for storing liquefied gas near atmospheric pressure. U.S. Patent US3191395 A, 1965.

DOI: 10.1021/acs.iecr.7b03633
Ind. Eng. Chem. Res. 2018, 57, 5903−5913